

SLAC-PUB-3114
RL 83-039
TUHEL 83-6
April 1983
(T/E)

CHARM PHOTOPRODUCTION CROSS SECTION AT 20 GeV*

SLAC Hybrid Facility Photon Collaboration

K.Abe^m, T.C. Bacon^e, J. Ballam^k, L. Berny^l, A.V. Bevan^e, H.H. Bingham^o, J.E. Brau^q, K. Braune^{k†}, D. Brick^b, W.M. Bugg^q, J. Butler^k, W. Cameron^e, J.T. Carroll^k, C.V. Cautis^k, J.S. Chima^e, H.O. Cohnⁱ, D.C. Colley^a, G. T. Condo^q, S. Dado^l, R. Diamond^d, P.J. Dornan^e, R. Erickson^k, T. Fieguth^k, R.C. Field^k, L. Fortney^c, B. Franek^j, N. Fujiwara^h, R. Gearhart^k, T. Glanzman^k, J. J. Goldberg^l, G.P. Gopal^j, A.T. Goshaw^c, E.S. Hafen^q, V. Hagopian^d, G. Hall^e, E.R. Hancock^j, T. Handler^q, H.J. Hargis^q, E.L. Hart^q, P. Haridas^q, K. Hasegawa^m, T. Hayashino^m, D.Q. Huang^{q††}, R. I. Hulsizer^q, S. Isaacson^l, M. Jobes^a, G.E. Kalmus^j, D.P. Kelsey^j, J. Kent^o, T. Kitagaki^m, J. Lannutti^d, A. Levy^p, P. W. Lucas^c, M. MacDermott^j, W.A. Mannⁿ, T. Maruyamaⁿ, R. Merenyiⁿ, R. Milburnⁿ, C. Milstene^p, K.C. Moffeit^k, J.J. Murray^k, A. Napierⁿ, S. Noguchi^h, F. Ochiai^f, S. O'Neale^a, A.P.T. Palounek^c, I.A. Pless^q, M. Rabin^{k†††}, P. Rankin^e, W.J. Robertson^c, A.H. Rogers^q, E. Ronat^r, H. Rudnicka^b, T. Sato^f, J. Schnepsⁿ, S.J. Sewell^j, J. Shank^o, A.M. Shapiro^b, C. K. Sinclair^k, R. Sugahara^f, A. Suzuki^f, K. Takahashi^f, K. Tamai^m, S. Tanaka^m, S. Tether^q, H.B. Waldⁿ, W.D. Walker^c, M. Widgoff^b, C.G. Wilkins^a, S. Wolbers^o, C.A. Woods^e, Y. Wu^q, A. Yamaguchi^m, R.K. Yamamoto^q, S. Yamashita^h, G. Yekutieli^r, Y. Yoshimura^f, G.P. Yost^o, H. Yuta^m

Submitted to Physical Review Letters

* Work supported by the Department of Energy, contract DE-AC03-76SF00515

- a. Birmingham University, Birmingham, England
- b. Brown University, Providence, Rhode Island, USA
- c. Duke University, Durham, North Carolina, USA
- d. Florida State University, Tallahassee, Florida, USA
- e. Imperial College, London, England
- f. KEK, Oho-machi, Tsukuba-gun, Ibaraki, Japan
- g. Massachusetts Institute of Technology, Cambridge, Massachusetts, USA
- h. Nara Womens University, Nara, Japan
- i. ORNL, Oak Ridge, Tennessee, USA
- j. Rutherford Appleton Laboratory, Didcot, England
- k. Stanford Linear Accelerator Center, Stanford University, Stanford, California, USA
- l. Technion-Israel Institute of Technology, Haifa, Israel
- m. Tohoku University, Sendai, Japan
- n. Tufts University, Medford, Massachusetts, USA
- o. University of California, Berkeley, California, USA
- p. University of Tel Aviv, Tel Aviv, Israel
- q. University of Tennessee, Knoxville, Tennessee, USA
- r. Weizmann Institute, Rehovot, Israel

ABSTRACT

Forty seven charm events have been observed in an exposure of the SLAC Hybrid Facility to a 20 GeV backward scattered laser beam. Thirty seven events survive all the necessary cuts imposed. Based on this number we calculate the total charm cross section to be (63^{+33}_{-28}) nb.

In this letter we present results on the charm photoproduction cross section in an experiment using the SLAC Hybrid Facility. Results on lifetimes of charmed particles based on part of the data were published earlier⁽¹⁾.

The SLAC 1m hydrogen bubble chamber was exposed to a 20 GeV photon beam produced by Compton scattering of laser light by the 30 GeV electron-beam. It was collimated to 3 mm in diameter. The photon beam energy spectrum is shown in Figure 1. It peaks at 20 GeV with a full width at half maximum of 2 GeV. Most of the data were taken at photon intensities of 20-30 γ /pulse. In order to detect decays of charmed particles, a fourth camera with high resolution optics having a resolution of 55 μm over a depth of field ± 6 mm was used. The cameras were triggered either on the passage of a charged particle through three multiwire proportional chambers and pointing back to the fiducial volume of the bubble chamber or on a sufficient energy deposition in an array of lead-glass blocks. Particle identification was provided by ionisation measurements in the bubble chamber and light detection in two large aperture Cerenkov counters. More details of the experimental setup and trigger are given in Ref. 1.

The results presented here are based on 270,000 hadronic interactions found in a restricted fiducial volume. All hadronic events were closely examined for the decays of short lived particles within 1 cm of the production vertex. When such a decay was found, the following cuts were applied to ensure that the decays which survived were genuine charm decays:

- (a) Decays with less than two charged products were rejected.
- (b) Two prong decays consistent either with photon conversions or strange particle hypotheses were rejected. To eliminate K^0 decays, the two body (assumed to be $\pi\pi$) invariant mass had to be greater than 550 MeV and also be more than 5 standard deviations above the K^0 mass in order to be accepted. Analogous criteria were used to remove $\Lambda, \bar{\Lambda} (m_{p\pi} < 1130\text{MeV})$ decays and $\gamma \rightarrow e^+e^- (m_{ee} < 50\text{MeV})$ conversions.

- (c) Three prong decays consistent either with $K^\pm \rightarrow \pi^\pm \pi^+ \pi^-$ or $\Sigma^+ \rightarrow p \pi^0 (\pi^0 \rightarrow e^+ e^- \gamma)$ were rejected as were the decays consistent with a neutral strange particle decay superimposed on a track from the production vertex.

We found 47 events with either one or two decays satisfying cuts (a) - (c) with 56 visible decays altogether. An example of one of these events is shown in Figure 2. We have investigated other possible sources of background which would simulate charmed particle decays, such as secondary interactions with one of the tracks undetected. These studies, based on calculations and also on searching for decay-like interactions at distances greater than 1 cm, show that backgrounds from all such sources combined are less than 3 % of the charm signal. The absence of any appreciable background can also be seen in Figure 3, where a histogram of the decay length L for all the 56 decays is shown, by noting that there are no decays satisfying cuts (a)-(c) observed beyond 5 mm. From the same figure, however, it is obvious that there is a loss of the charm signal at small L.

The sensitivity (measured in events /nb) of the experiment, based on the total photon flux and scanning and triggering efficiencies, was determined as follows. The incident photon flux was determined by summing the signals from a lead-lucite shower counter positioned in the beam downstream of the bubble chamber. The signals from this counter were accumulated for all beam pulses for which the cameras were ready to trigger. This counter was calibrated using e^+e^- pairs observed in the bubble chamber, and in a pair spectrometer upstream of the bubble chamber. Charm event triggering efficiency was determined by taking every 50th frame of film untriggered during the course of the experiment. From this data we determined the trigger efficiency for ordinary hadronic events as a function of charge multiplicity and then deduced the charm triggering efficiency from the multiplicity distribution of charm events, giving $92 \pm 4\%$. This value is consistent with independent Monte Carlo studies. Scanning efficiency for

charm events was determined by scanning the film twice. Based on the events passing the cuts discussed below we determine this to be $95^{+4}_{-10}\%$.

From the above we calculate the sensitivity to be $2.09^{+0.21}_{-0.29}$ events/nb. This number was checked by comparing the total number of hadronic interactions found in the same sample of film to the total hadronic cross section; this calculation gives consistent results.

As a first important, completely model independent, result we calculate the lower limit to the charm cross section. Using the 47 events found and the sensitivity, we find (with 90 % confidence) the charm cross section to be greater than 16.7 nb.

In order to determine the charm cross section, σ_c , it is necessary to correct for the events removed by the cuts (a)-(c) or undetected such as those where both charmed decays occur very close to the production vertex. Further cuts were applied to ensure that only events detected with uniform and high efficiency were used. These cuts were:

- (d) A minimum decay length cut of $500 \mu\text{m}$ was imposed.
- (e) An impact distance, defined as the minimum distance between the extrapolated track and production vertex in the plane of the view, d_{max} , greater than $110 \mu\text{m}$ (2 track widths) was required for at least one track in a decay.
- (f) An impact distance, d_2 , greater than $40 \mu\text{m}$ was required for a second track from the same decay vertex.

After imposing these cuts, 37 events remained with one or two decays satisfying all the cuts. There are 40 such decays and their decay length distribution is shown in the shaded histogram of Figure 3. (The turnover at small length is a consequence of cuts (e) and (f).) These include 15 neutral (7 four-prongs and 8 two-prongs), 6 positive (all three-prongs), 13 negative (all three-prongs) and 6 charge/neutral ambiguous. Five of the neutral and 9 of the charged decays are compatible with Cabibbo-allowed D decays with no missing neutral particles; the rest are compatible if missing π^0 's, K^0 's or ν are assumed. In most cases not all charged particles are identified. Thus for most D^\pm candidates, the F^\pm hypothesis cannot be excluded, and for some the Λ_c^+ is also possible.

To calculate σ_c , the number of charm events has to be corrected for the effect of the cuts (a) - (f). This correction depends on the production mechanism of the charmed particle pairs, the decay mechanism such as branching ratios into various decay channels, and lifetimes. In order to estimate its value, charmed particle events were generated by a Monte Carlo program and cuts (a)-(f) were applied to the generated events. Several different production mechanisms were considered and the decay modes and branching ratios assumed were taken from Ref. 2. For the production mechanisms considered the final result is only weakly dependent on the momentum spectrum of the charmed particles, and therefore on the details of the dynamics of the process. On the other hand, it is quite sensitive to the decay characteristics, particularly the lifetimes and branching ratios, and consequently depends on the type of charmed particle pairs produced.

It is difficult to determine experimentally the relative production rates of the various possible types of charmed particle pairs produced. This is because only one decay is observed in most events and because most of the observed charged decays are not uniquely identified as D's, F's or Λ_c 's. We therefore estimated σ_c by considering extreme, yet plausible, pair production models. Using the values $\tau_D \pm = 8.2^{+4.5}_{-2.5}$ and $\tau_{D^0} = 6.7^{+3.5}_{-2.0} \times 10^{-13}$ sec, as determined in our experiment (1), and $\tau_{\Lambda_c} = 2.0 \times 10^{-13}$ sec, we obtain the following results for the models considered: (1) 52.1 nb for $\gamma p \rightarrow \bar{D} DN(\pi)$, (2) 47.9 nb for $\gamma p \rightarrow \bar{D}^* DN(\pi)$; (3) 80.5 nb for $\gamma p \rightarrow \bar{D} \Lambda_c^+(\pi)$ and (4) 93.2 nb for $\gamma p \rightarrow \bar{D} \Sigma_c^{++}(\pi)$. The uncertainties in these values are +40 %, -30 %. Taking into account these systematic errors due to production and decay uncertainties, and using a median value based on the assumption of equal mixture of the two extreme models (2 and 4) we obtain the total charm cross section to be:

$$\sigma(\gamma p \rightarrow \text{CHARM}) = (63^{+33}_{-28}) \text{nb}$$

A second approach was also tried, in which each of the 40 decays passing all cuts

was assigned a momentum and decay multiplicity dependent weight. This calculation assumed that the decaying particle was a "D meson". This method requires no assumptions as to the dynamics of "D meson" production, relative production rates of charged and neutrals or relative multiprong decay branching ratios. Making the same assumption about the types of charmed particles produced this approach gives cross section values consistent with those of the first method.

In Figure 4 we show our measurement together with measurements from other experiments and also some theoretical predictions for the cross section dependence on beam energy. Of these, the results favor the Photon Gluon Fusion models.

We wish to thank the SLAC bubble chamber crew for their dedication and performance under difficult conditions, particularly for the work on the High Resolution Camera. We are especially indebted to the film scanners for their efforts in finding the events.

This work was supported by the Japan-US Cooperative Research Project on High Energy Physics under the Japanese Ministry of Education, Science and Culture; the US Department of Energy; the Science and Engineering Research Council (UK); the US National Science Foundation; the US-Israel Binational Science Foundation; and the Israel Academy of Sciences Commission for Basic Research.

REFERENCES

† Max Kade Foundation Fellow.

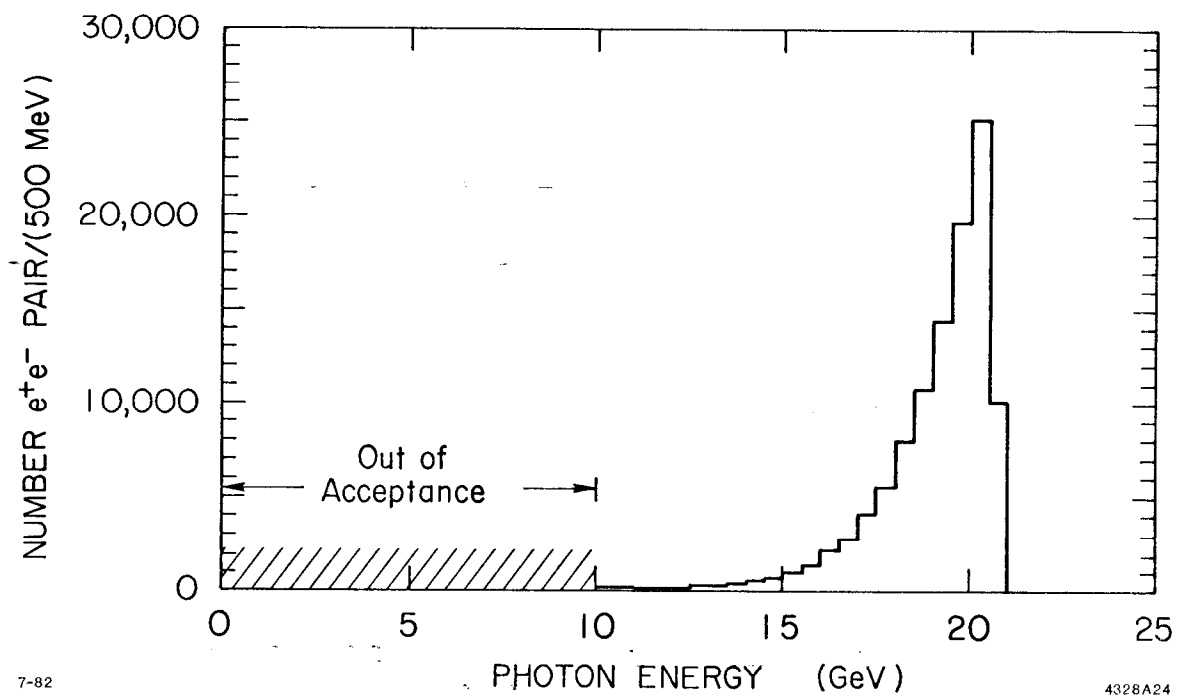
†† On leave of absence from the Institute of High Energy Physics, Beijing, China

††† Permanent address: University of Massachusetts, Amherst, Mass. 01003

1. K. Abe et al., Phys. Rev. Lett. 48, 1526 (1982).
2. G. Trilling, Phys. Rep. 75, 57 (1981)
3. F. Halzen and D. M. Scott, Phys. Lett. 72B, 404, (1978); H. Fritzsche and K. M. Streng, Phys. Lett. 72B, 385, (1978); V. A. Novikov, M. A. Shifman, A. I. Vainshtein and V. I. Zakharov, N. P. B136, 125, 1978; J. Babcock, D. Sivers and S. Wolfram, Phys. Rev. D18, 162, 1978.
4. D. Aston et al., Phys. Lett. 94B, 113 (1980), P. Avery et al, Phys. Rev. Lett. 44, 1309 (1980), J. J. Russell et al, Phys. Rev. Lett. 46, 799 (1981), J. J. Aubert et al., Nucl. Phys. B213 (1983) 31-64, A. R. Clark et al., Phys. Lett. 45, 682 (1980)

FIGURE CAPTIONS

1. Photon energy spectrum as measured by the pair spectrometer.
2. An example of a charm event.
3. Decay length distribution of charm decays.
4. Theoretical predictions for the total charm photoproduction cross section as a function of photon energy (see Ref. 3). Our result is shown together with results from other experiments. (Ref 4)



7-82

4328A24

FIGURE 1

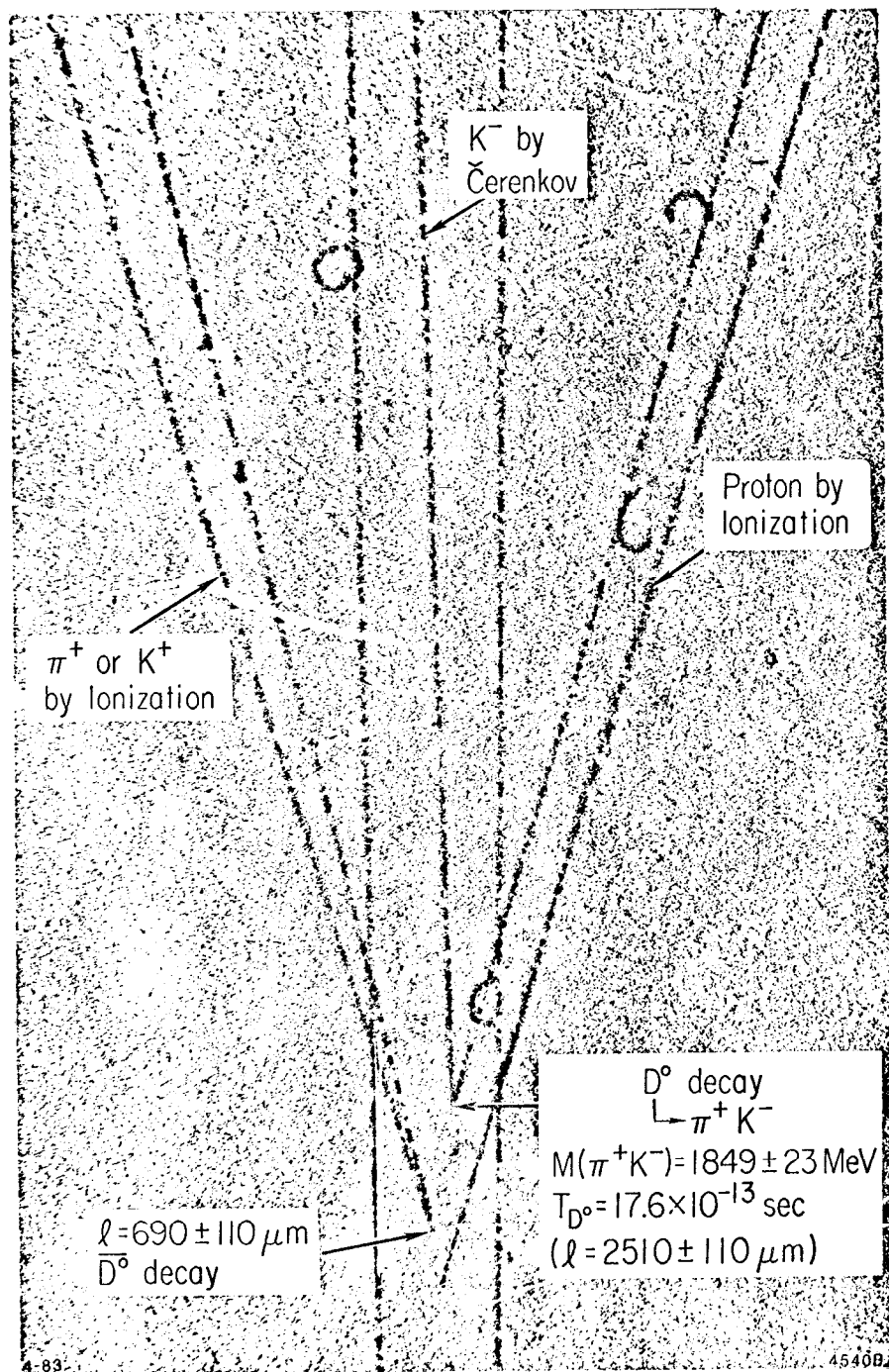
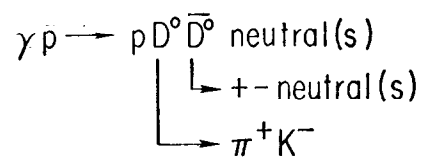


FIGURE 2

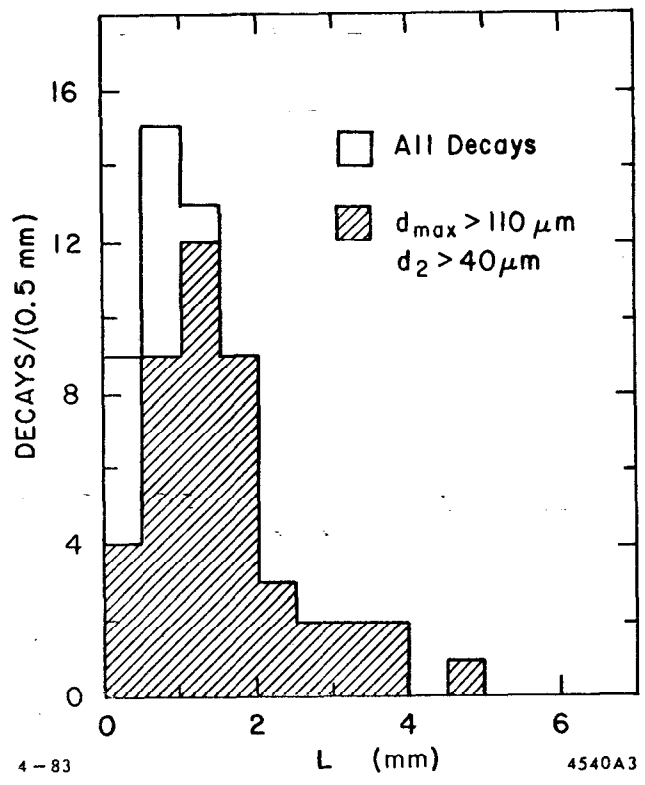


FIGURE 3

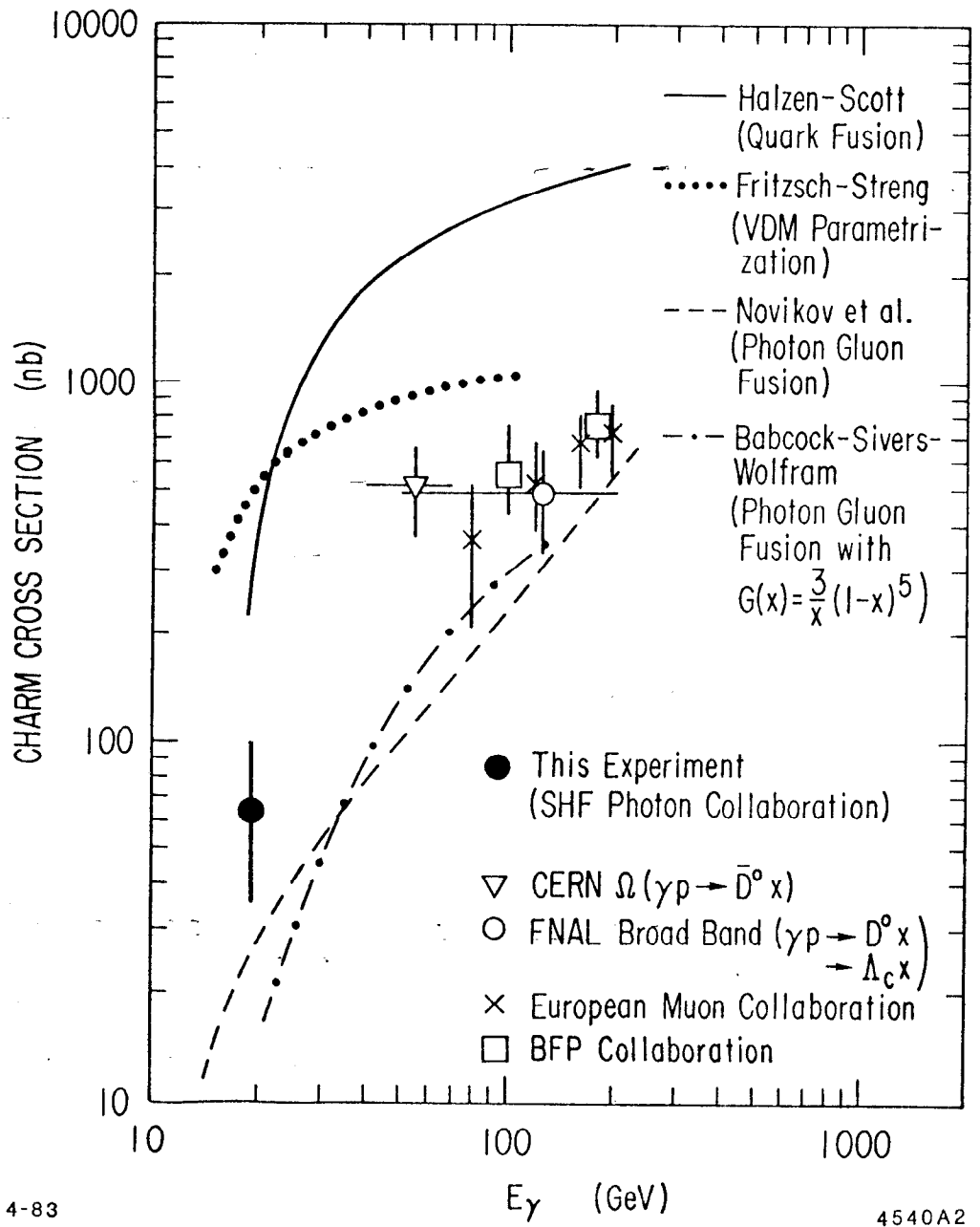


FIGURE 4